SAND79-1480
Unlimited Release
UC-80

MASTER

Sandia Pulsed Reactor Facility (SPRF) Calculator-Assisted Pulse Analysis and Display System

Berry F. Estes, Donald T. Berry

SF 2900 Q(7-73)

CONTENTS

ILLUSTRATIONS

TABLES

SANDIA PULSED REACTOR FACILITY (SPRF)
CALCULATOR-ASSISTED PULSE ANALYSIS AND DISPLAY SYSTEM

CHAPTER 1. INTRODUCTION

The two reactors (SPR II and SPR III) at Sandia Laboratories Pulsed Reactor Facility are solid-metal, fast-burst-type reactors and as such can operate at high powers for very short periods of time (short Full Width Half Maximum, FWHM). Since start-up of the reactors, oscilloscopes have been used to record (by camera) the pulse shape and log N systems used to determine period. Virtually no other pulse information is available. A decision was made to build a system that could collect the basic input data available from the reactor--fission chambers, photodiodes, and thermocouples--condition the signals, and output the various parameters such as power, energy, temperature, period, and lifetime on hard copy that would be available as a record for operations personnel and the experimenter. Because the reactors operate in short time frames (pulse operation), it is convenient to utilize the classical Nordheim-Fuchs approximation of the diffusion equation to describe reactor behavior. This report describes the work performed to develop the calculator system and analytical models for calculating the desired parameters.

CHAPTER 2. DESCRIPTION

2.1 Reactor Site

The SPR Facility consists of the reactor building (KIVA), an instrument building, an earth-covered beam catcher building, support structures, and equipment. The reactor control room is located about 61 m to the northeast of the reactor building, outside an exclusion area defined by a double security fence. Figure 2.1-1 shows the general layout of the facility.

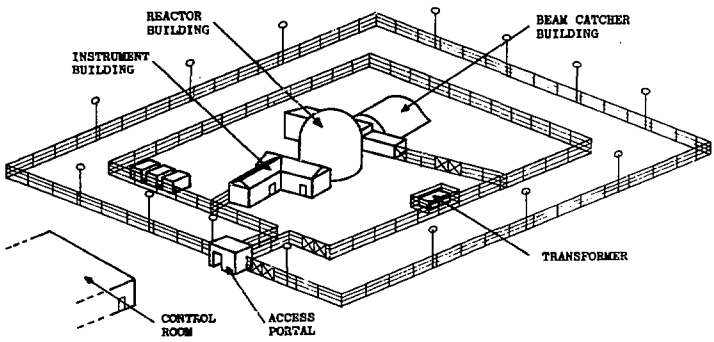

Figure 2.1-1. General Layout of the SPR Inner Exclusion Area

2.2 Sandia Pulsed Reactor II (SPR II)

The SPR II, operational since 1967, is designed to provide a "point" source of near-fission spectrum neutrons. It is a bare, unreflected, and unmoderated cylindrical assembly of 10 w/o molybdenum and 90 w/o uranium enriched to 93% in ^{235}U. The core is partitioned into six stacked fuel rings divided into two groups of three rings each. The upper group is stationary, while the lower group moves over a 5.08-cm vertical range. This lower core half, the "Safety Block," provides the primary shutdown mechanism for terminating a nuclear operation. Four vertical holes in the core accommodate three control rods and a burst rod. A central experiment cavity extends through both core halves; it is at the horizontal mid-plane of this chamber that the maximum design fluence of 1.0×10^{15} n/cm^2 can be achieved over the time interval of a 450°C (ΔT) burst. Neutron fluence, flux, and gamma dose values for the standard yield pulse (300°C) are shown in Table 2.2-1.[1] The total fuel mass of SPR II is ≈ 106 kg. See Figure 2.2-1 for a side view of the SPR II core and Figure 2.2-2 for a side view of the reactor and its support structure. Note in Figure 2.2-3 the relative locations of the central experiment cavity and the four surrounding holes for control and burst rods. Graphical information regarding burst size, energy spectra, and spacial flux distribution is included in Figures 2.2-4 through 2.2-7.

TABLE 2.2-1

SPR II Typical Values for 300°C ΔT Pulse

	Glory Hole (max)	15.2 cm From Centerline (=shroud surface)	30.5 cm From Centerline
Φ(>3 MeV) nvt	7.1×10^{13}	8.3×10^{12}	1.9×10^{12}
Φ(>10 keV) nvt	7.1×10^{14}	5.9×10^{13}	1.4×10^{13}
FWHM (μs)	52	52	52
Φ(>3 MeV) nv	1.4×10^{18}	1.6×10^{17}	3.6×10^{16}
Φ(>10 keV) nv	1.4×10^{19}	1.1×10^{18}	2.7×10^{17}
Gamma (rads)	1.2×10^{5}	1.6×10^{4}	3.6×10^{3}
Gamma rate (rads/s)	2.3×10^{9}	3.1×10^{8}	7.2×10^{7}

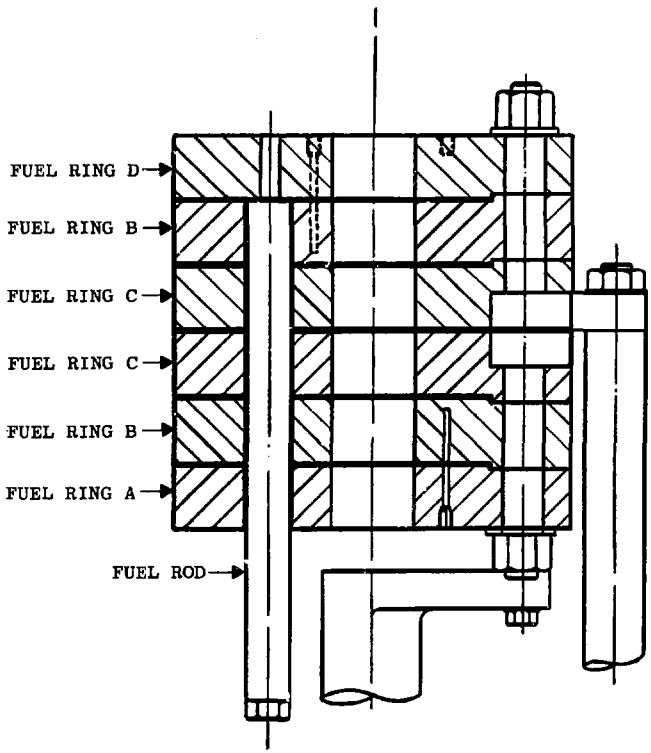

Figure 2.2-1. SPR II Core, Side View

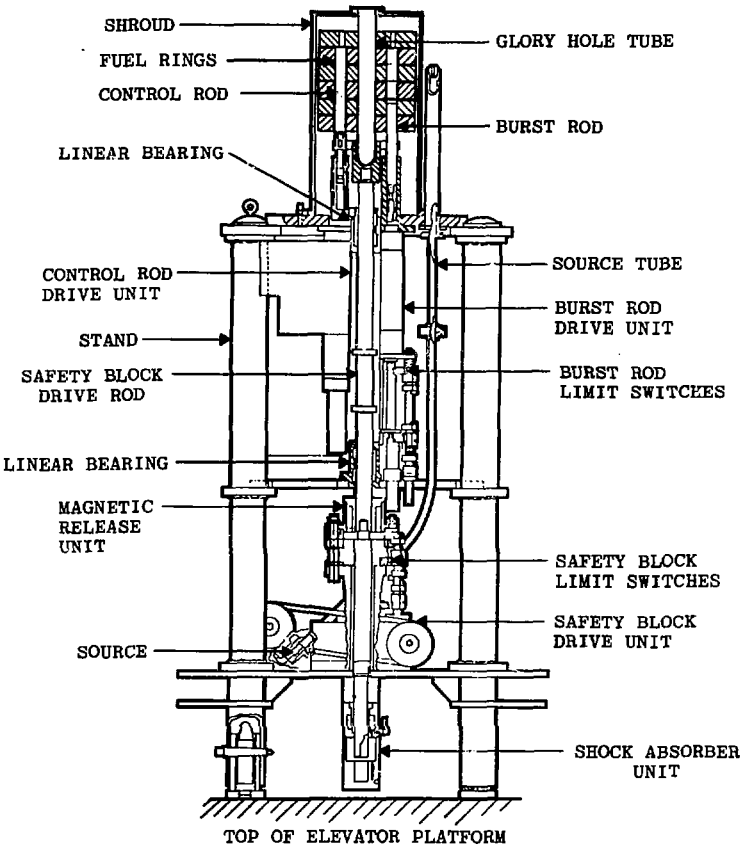

Figure 2.2-2. SPR II Core and Support Structure

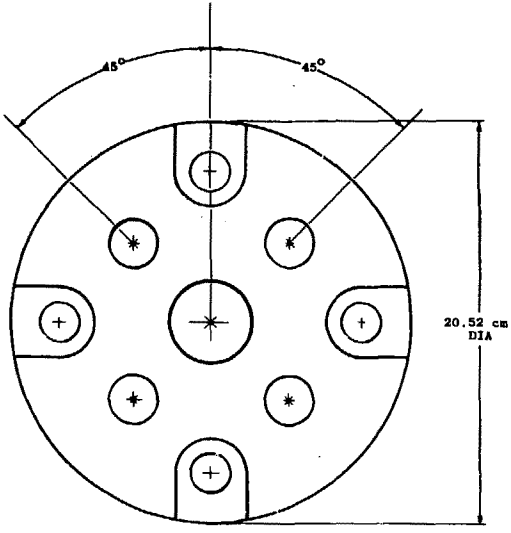

Figure 2.2-3. SPR II Fuel Plate "B"

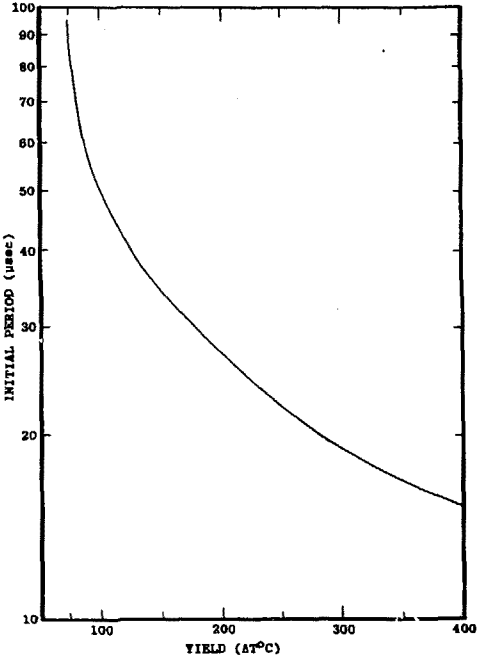

Figure 2.2-4. SPR II Initial Period vs Pulse Yield

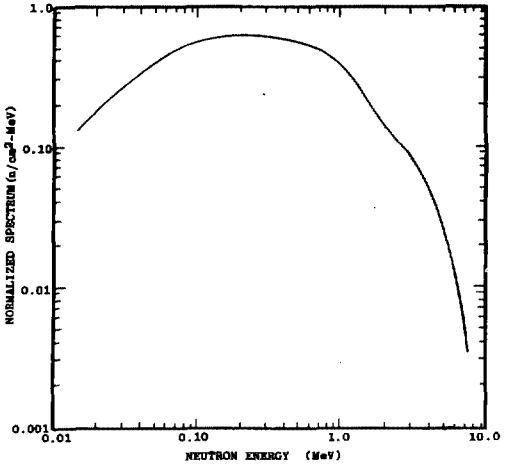

Figure 2.2-5. SPR II Normalized Differential Neutron Energy Spectrum

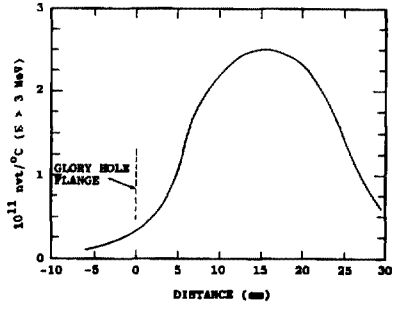

Figure 2.2-6. SPR II Axial Fluence ≥ 3 MeV/°C

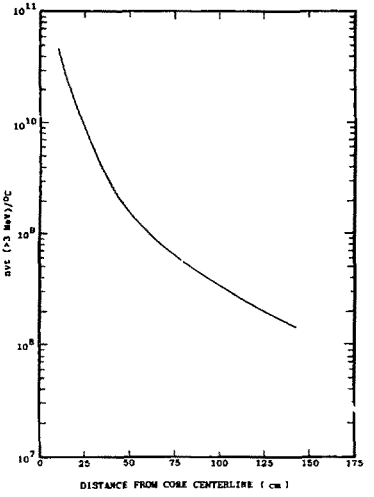

Figure 2.2-7. SPR II Leakage Fluence ≥3 MeV/°C

2.3 Sandia Pulsed Reactor III (SPR III)

On line since 1975, SPR III incorporates several design improvements over its predecessor. Foremost is an enlarged central experiment cavity offering 44 times the volume of the SPR II "Glory Hole." The fuel mass of SPR III is about 258 kg, the fuel material being identical to that of the SPR II. The core is also divided into two halves, but SPR III consists of a total of 18 fuel rings and the safety block ranges 8.89 cm between its full down position and the mating position. Instead of internally positioned control and burst rods, SPR III controls reactivity with four externally-mounted reflector elements: one aluminum burst element and three copper control elements. The maximum design fluence at the core horizontal midplane is 6×10^{14} nvt for a 450°C ΔT burst operation. Neutron fluence, flux, and gamma dose values for the standard yield pulse 300°C ΔT are shown in Table 2.3-1.[1] Figure 3.2-1 shows a side view of the SPR III fuel assembly; a view of the reactor and its associated support structure is shown in Figure 2.3-2. Figure 2.3-3 shows the relative

locations of the experiment cavity and the four reactivity control elements. Graphical data with regard to burst size, energy spectra, and spacial flux distribution is also included in Figures 2.3-4 through 2.3-6.

TABLE 2.3-1

SPR III Typical Values for 300°C ΔT Pulse

	Glory Hole (max)	30.5 cm From Centerline	63.5 cm From Centerline
Φ(>3 MeV) nvt	5.38×10^{13}	6.80×10^{12}	1.57×10^{12}
Φ(>10 keV) nvt	4.57×10^{14}	4.90×10^{13}	1.13×10^{13}
FWHM (μs)	90	90	90
Φ(>3 MeV) nv	5.98×10^{17}	7.56×10^{16}	1.74×10^{16}
Φ(>10 keV) nv	5.08×10^{18}	5.44×10^{17}	1.25×10^{17}
Gamma (rads)	1.31×10^{5}	1.36×10^{4}	2.04×10^{3}
Gamma rate (rads/s)	1.46×10^{9}	1.73×10^{8}	2.26×10^{7}

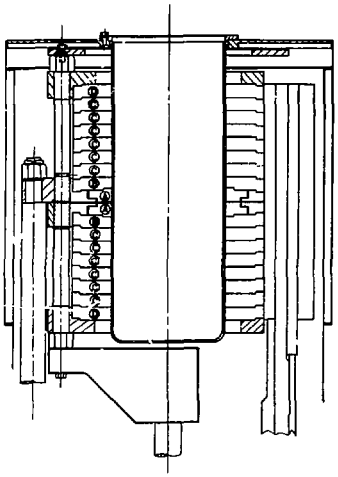

Figure 2.3-1. SPR III Core, Side View

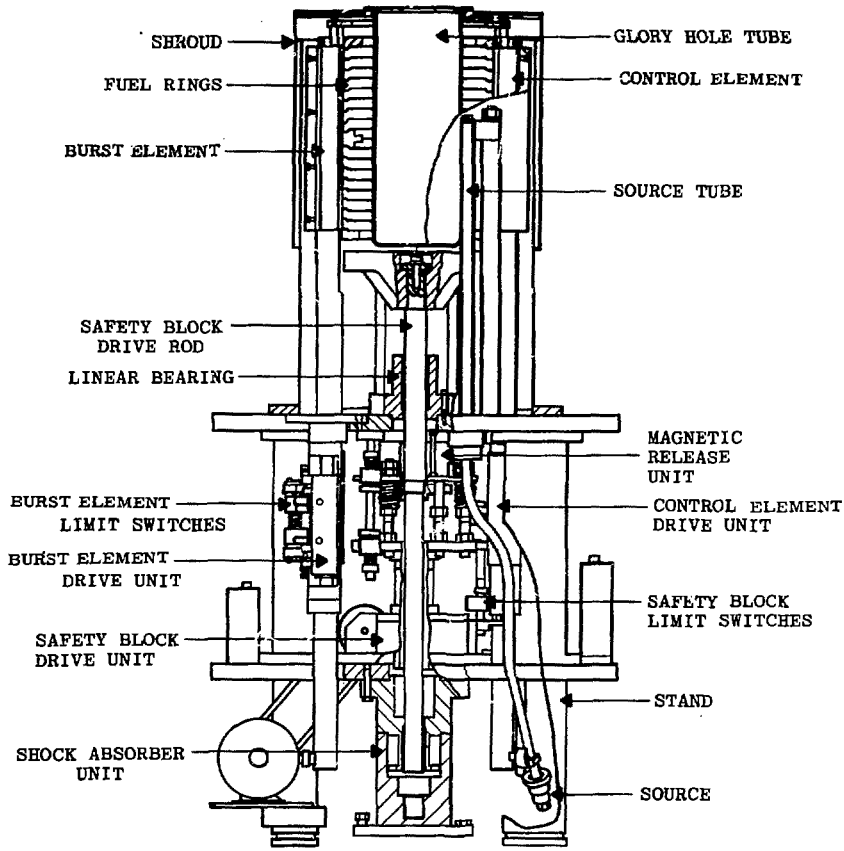

Figure 2.3-2. SPR III Core and Support Structure

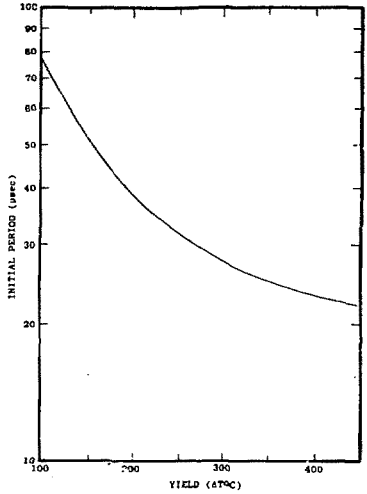

Figure 2.3-3. SPR III Initial Period vs Pulse Yield

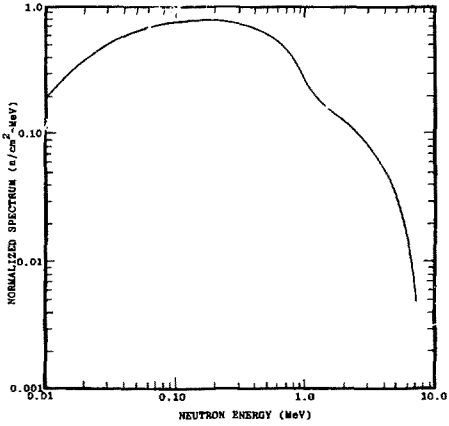

Figure 2.3-4. SPR III Normalized Differential Neutron Energy Spectrum

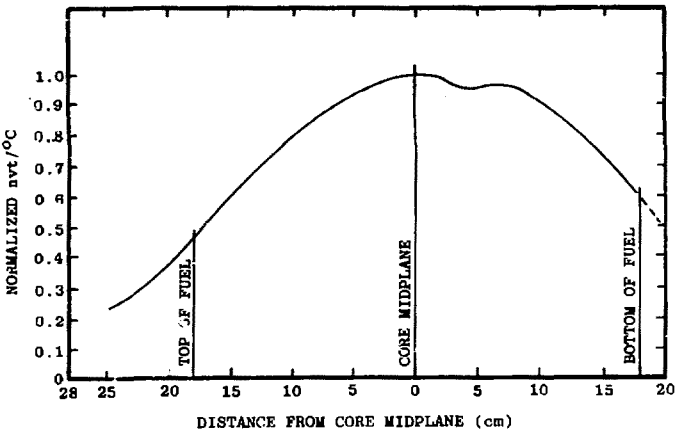

Figure 2.3-5. SPR III Axial Fluence ≥3 MeV/°C

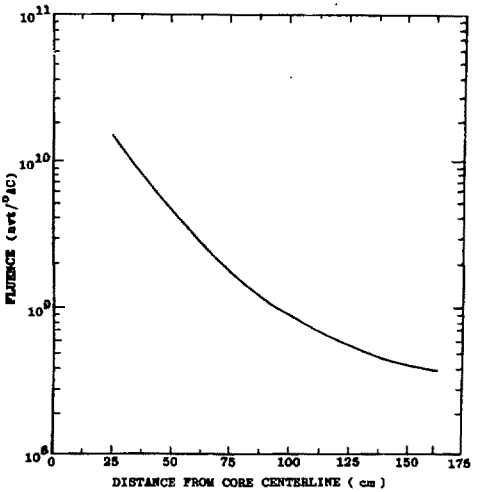

Figure 2.3-6. SPR III Leakage Fluence ≥3 MeV/°C

2.4 Calculator and Peripherals

The data acquisition system collects information from a primary source (neutron detector) and analyzes the data for the purpose of calculating certain parameters. The system consists of two A-D converters, one calculator and one x-y plotter. The calculator is a Hewlett Packard Model 9825A desk-top device which offers flexibility in both software potential and controller applications. Some of the features that characterize the unit are its high speed direct memory access of 400 K 16-bit words per second, a two-track, bidirectional memory tape, and a wide calculation range ($\pm 10^{511}$ to $\pm 10^{-511}$). Plug-in style Read Only Memories (ROMs) extend the software capabilities of the basic calculator. Those used in the SPR system include a plotter ROM, both a general and an extended input/output ROM to provide complete peripheral interface control, a string variable ROM to permit operations with letters and words, an advanced programming ROM, and a matrix ROM. A 16-character thermal strip printer offers a hard-copy output, while a 32-character LED display lends itself to rapid program line editing.

High-resolution graphical output is obtained by using a Hewlett Packard Model 9872A microprocessor-based plotter. With pen movements as small as 0.025 mm and a choice of a number of pen speeds, the quality of the graphics product is quite good. The maximum plotting area available is 40 x 28 cm.

Taking a voltage signal from standard photodiode or fission chamber detectors are two waveform recorders (Model 805, Biomation Corporation). The recorders act as digitized pulse data storage devices, holding information for later nondestructive access by either the calculator or an on-line CRT display (the recorders are equipped with an internal D/A converter). A complete sweep of the recorder acquires 2048 data points at a rate determined by an internal crystal oscillator. A sample interval selector switch provides 18 discrete time choices between 0.2 μs and 0.1 s. Similarly, nine levels of signal sensitivity are available, ranging from 100 mV to 50 V with 8 bits (1 part in 256) resolution of all sample rates. Because the recorder continues to sample when the trigger

signal is absent, the trigger itself can be established as an intermediate location of the recorded waveform, thereby allowing an entire pulse to be captured. That is, data prior to the trigger can also be saved by adjusting the fraction of the 2048 samples taken between the trigger and the end of recording.

A diagram of the SPR data acquisition system is provided in Figure 2.4-1.

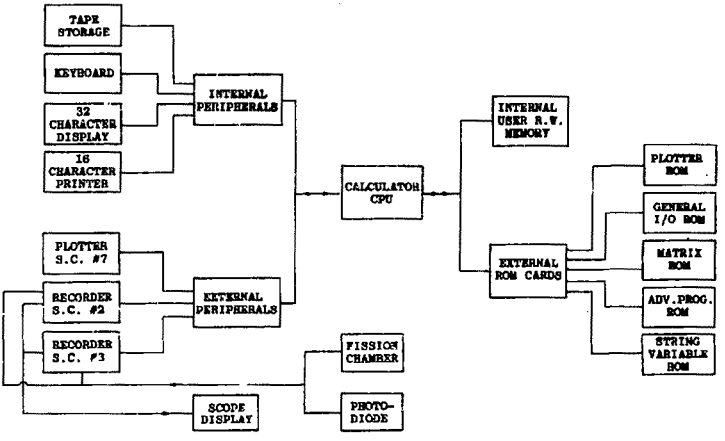

Figure 2.4-1. SPR Data Acquisition System

CHAPTER 3. FUNDAMENTAL CALCULATIONS

3.1 Nordheim-Fuchs Model With Variable Heat Capacity

The kinetic behavior of a reactor core is strongly influenced by the delayed neutrons. The time-dependent behavior of a reactor, considering the one energy group model, can be described by the general form of the diffusion equation[2]

$$D\nabla^2\phi - \Sigma_a\phi + S = \frac{dn}{dt} \tag{1}$$

where $\phi = nv$.

The source term can be defined as:

$$S = \text{(prompt neutrons)} + \text{(six groups of delayed neutrons)} \tag{2}$$

$$= \kappa_\infty \Sigma_a \phi(1 - \beta) + \sum_{i=1}^{6} \lambda_i C_i \tag{3}$$

Substitution of Eq 3 into Eq 1 yields the following time-dependent equation of neutron behavior:

$$D\nabla^2\phi - \Sigma_a\phi + \kappa_\infty \Sigma_a (1 - \beta) + \sum_{i=1}^{6} \lambda_i C_i = \frac{dn}{dt} \tag{4}$$

where

ϕ = monoenergetic neutron flux
D = diffusion coefficient
Σ_a = macroscopic absorption cross section
κ_∞ = infinite multiplication factor
β = delayed neutron fraction
λ = radioactive decay constant
C_i = concentration of delayed neutron precursors
n = neutron density

Using the following relationships for the prompt neutron generation time, ℓ^*, and reactivity, ρ, Eq 4 can be simplified as follows:

$$\ell^* = \frac{1}{K_\infty v \Sigma_a} \tag{5}$$

$$\rho = \frac{K_{eff} - 1}{K_{eff}} \tag{6}$$

where

v = average neutron velocity

$$K_{eff} = \frac{K_\infty}{1 + B^2L^2} \tag{7}$$

Substituting * and for the equivalent terms and by letting $\nabla^2 = -B^2\phi$ and $D/\Sigma a = L^2$ reduces Eq 4 to

$$\frac{dn}{dt} = \frac{\rho - \beta}{\ell^*} n + \sum_{i=1}^{6} \lambda_i C_i \tag{8}$$

The companion equation for the time-dependent neutron precursors is given by

$$\frac{dC_i}{dt} = \beta_i K_\infty \sum_a \phi - \lambda_i C_i = \frac{\beta i}{\ell^*} n - \lambda_i C_i \tag{9}$$

The foregoing coupled differential equations apply to the general reactor condition, wherein the duration of the operation is long compared to the generation time of all neutrons (i.e., both prompt and delayed neutrons). Considering those operations that take place in a very short time as compared to the delayed neutron generation time, the above equations (Eqs 8 and 9) may be modified by considering that all neutron sources, except the production of prompt neutrons, can be neglected.

The resultant equation describing neutron behavior is given by

$$\frac{dn}{dt}\rho = \frac{\rho - \beta}{\ell^*} n \tag{10}$$

which is generally referred to as the Nordheim-Fuchs model. The reactivity input for this condition is given by

$$\rho = \rho_o - \alpha T \tag{11}$$

where

ρ_o = initial input reactivity
α = negative of the temperature coefficient of reactivity.
T = core averaged full temperature

Further, if it is assumed that the heating of the core is rapid enough to ignore heat losses, the adiabatic model for temperature can be given as

$$\frac{dT}{dt} = \frac{n}{C} \tag{12}$$

where

T = temperature rise
C = specific heat capacity.

If the heat capacity is assumed to be a linear function of temperature, the following expression can be used to describe the heat capacity:

$$C = C_o + \gamma T \tag{13}$$

Combining Eqs 10, 11, 12 and 13 results in the following:

$$\frac{dn}{dt} = \frac{\rho_o - \alpha T - \beta}{\ell^*} n \tag{14}$$

$$\frac{dT}{dt} = \frac{n}{C_o + \gamma T} \quad . \tag{15}$$

The independent variable can be changed thus,

$$\frac{dn}{dt} \cdot \frac{dT}{dT} = \frac{dn}{dT} \cdot \frac{dT}{dt}$$

or

$$\frac{dn}{dt} \cdot \frac{n}{C_o + \gamma T} = \frac{\rho_o - \alpha T - \beta}{\ell^*} n$$

$$\frac{dn}{dT} = \frac{(\rho_o - \alpha T - \beta)(C_o + \gamma T)}{\ell^*}$$

$$\frac{dn}{dT} = \frac{1}{\ell^*} \left\{ C_o(\rho_o - \beta) + \left[(\rho_o - \beta)\ \gamma - C_o\alpha \right]\ T - \alpha\gamma T^2 \right\} \tag{16}$$

which is the general differential equation for relating power (n) to temperature (T). Integrating Eq 16 yields the following first integral general solution for power as a function of temperature with variable heat capacity:

$$n - n_o = \frac{C_o(\rho_o - \beta)}{\ell^*} T + \frac{\left[(\rho_o - \beta) - C_o\alpha \right]}{2\ell^*} T^2 - \frac{\alpha\gamma}{3\ell^*} T^3 \quad . \tag{17}$$

3.2 Temperature and Power Relationships

The temperature of the core at time of peak power is a parameter of interest in development of particular power equations, namely, an expression for peak power. Differentiating Eq 17 and setting the result equal to zero yields the temperature occurring at the time the peak power occurs. Thus,

$$\frac{dn}{dT} = \frac{1}{\ell^*} \left\{ C_o(\rho_o - \beta) + \left[(\rho_o - \beta)\ \gamma - C_o\alpha \right] T - \alpha\gamma T^2 \right\} \tag{18}$$

and recalling that the solution to the quadratic equation is

$$X = \frac{-b \pm \sqrt{b^2 - 4ac}}{2a}$$

the expression for temperature at peak power is given by

$$T(\hat{n}) = W = \frac{\rho_o - \beta}{\alpha} \quad . \tag{19}$$

Note: The second root yields $T(\hat{n}) = C_o/\alpha$ which is for the shutdown case and is not used for this solution.

Rewriting Eq 17 and combining terms results in

$$n - n_o = \frac{C_o(\rho_o - \beta)}{\ell^*} T - \frac{C_o\alpha}{2\ell^*} T^2 + \frac{(\rho_o - \beta)\gamma}{2\ell^*} T^2 - \frac{\alpha\gamma}{3\ell^*} T^3 \tag{20}$$

and substituting the temperature at peak power expression,

$$\hat{n} - n_o = \frac{C_o(\rho_o - \beta)}{\ell^*} W - \frac{C_o(\rho_o - \beta)}{2\ell^*} W + \frac{(\rho_o - \beta)\gamma}{2\ell^*} W^2 - \frac{\alpha\gamma}{3\ell^*} \left(\frac{\rho_o - \beta}{\alpha} \right) W^2$$

$$\hat{n} - n_o = \frac{C_o(\rho_o - \beta)}{2\ell^*} W + \frac{(\rho_o - \beta)\gamma}{6\ell^*} W^2 \tag{21}$$

or since

$$\hat{\eta} \gg \eta_o$$

$$\hat{\eta} = \frac{\rho_o - \beta}{*} \frac{C_o}{2} W + \frac{\gamma}{6} W^2 \tag{22}$$

which for the constant specific heat capacity case reduces to

$$\hat{\eta} = \frac{C_o W^2}{2 * \ell} \tag{23}$$

Utilizing the following substitutions that are defined for and applicable at peak power (i.e., $\rho = \beta$):

$$\rho = \beta = \rho_o - \alpha T \tag{24}$$

$$\tau(\text{period}) \quad \frac{\ell *}{\rho_o - \beta} \tag{25}$$

The expression for peak power can be rewritten as

$$\hat{\eta} = \frac{CW}{4} \tag{26}$$

Equation 26 is the expression for peak power that is used in the calculator program (see Section 3.3).

3.3 Data Processing Routine

A brief description of the software currently driving the calculator and peripherals is detailed in the flow diagram included as Figure 3.3-1. Under normal procedure, the waveform recorder parameters are selected in advance of the burst operation. Each recorder's sensitivity is set differently to assure data acquisition over a range of pulse yields. Once the data has been taken, the calculator program offers the operator the option of recording data on the tape cartridge so as to permit later analysis. In the event there is an offset or bias in the data the operator may list the first 25 data entries and make a corresponding adjustment to all values before the storage of the information on tape. In place of, or following, storage the operator can elect to plot the data either from a tape file or directly from the waveform recorder. A heading block names the reactor used, the experimenter, the date, the time of burst, and, after additional calculations initial reactor period, full-width half-maximum, yield as delta T (°C), and a conversion factor to scale the ordinate in units of gigawatts. By entering the waveform recorder time base setting, the operator initiates the period discrimination routine in which the matrix address of the peak power is found as well as the locations of $\hat{\eta}/3$ and $\hat{\eta}/8$. Subsequently, a linear regression is performed on the natural logarithms of the amplitudes within this interval; the slope of this line is the initial reactor period and is printed out. If this calculation differs sufficiently from the readings of two external analog devices, the operator can substitute a value in which he has more confidence and the calculation proceeds with the substitute. Peak power in watts is computed from the Nordheim-Fuchs model

$$\hat{\eta} = \frac{C \; T_{max}}{4T} \quad .$$

where T_{max} is the calculated temperature at peak power.

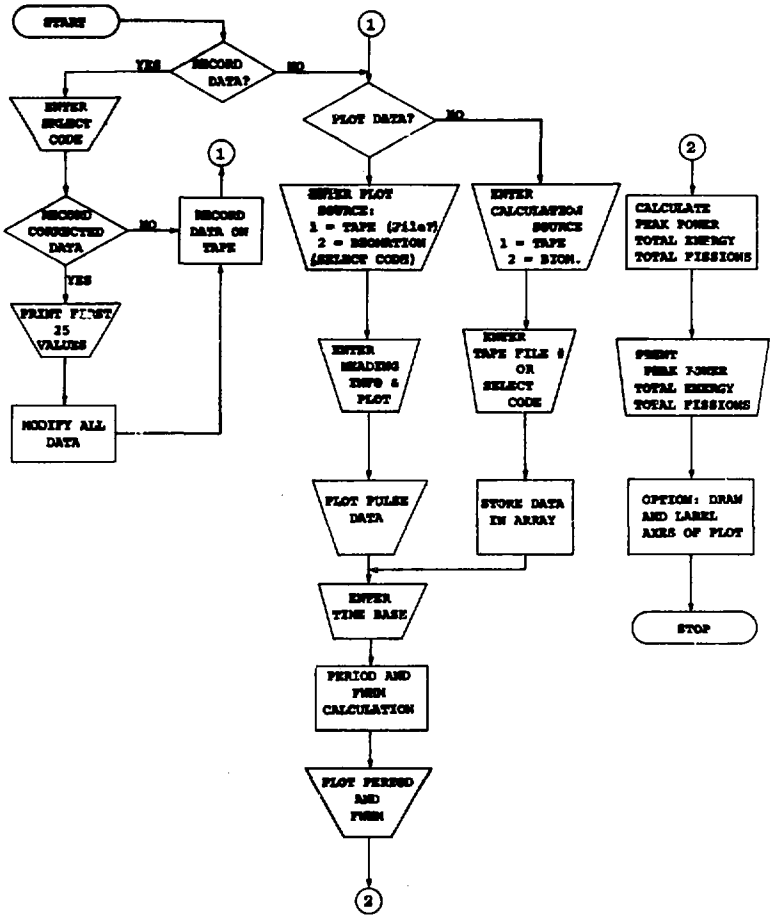

Figure 3.3-1. Peripherals Control Flow Diagram for Pulse Analysis Routine

Full-width half-maximum is determined by comparing addresses of the two $\eta/2$ points and using the known sampling rate. An integration subroutine is used to determine the total energy deposition from which the total number of fissions is calculated. Finally, the operator can choose to apply labeled axes to the plot. From an earlier search, the location of the peak is known. The vertical axis is drawn through this point and time in microseconds is marked off with this axis acting as a zero reference. For ease in reading off values, the vertical axis is always picked off according to the design of the graph paper used (20 units to the 1/2 in.) and a conversion factor is calculated and displayed on the plot to arrive at power in gigawatts. A sample plot made from a typical burst operation on SPR II is shown in Figure 3.3-2.

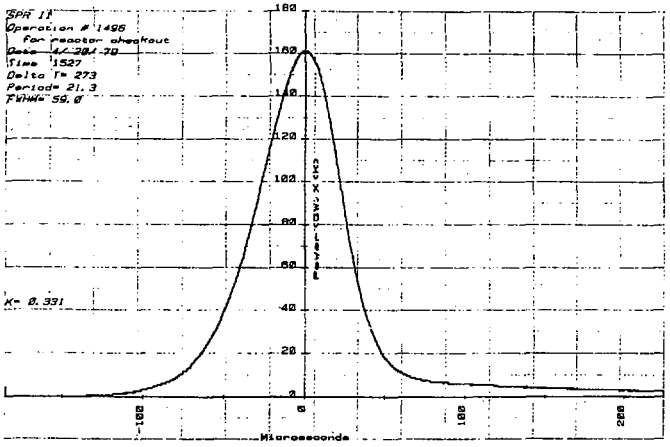

Figure 3.3-2. Typical Plot of a SPR II Pulse

CHAPTER 4. POTENTIAL APPLICATIONS

4.1 Passive Mode

Up to the present time, the calculator system has been used as an adjunct to the reactor, reducing data rapidly and providing the experimenter with a high-resolution graphical record of each burst operation. The format now in use is, in large part, a result of requests from users and will continue to change as more people are introduced to the system. Recently, for instance, a program was developed to quickly establish the distances from the reactor of many small experimental packages, each requiring a different dose during the same burst. Work is continuing on the refinement of a technique which checks the amount of control rod correction that is applied to deliver a pulse of any desired magnitude. Difficulties arise from the variety of reactivity effects seen by the burst element when perturbed by the mass and/or material makeup of the experiment considered. Other computational routines will include a determination of the static worth of an experiment as well as predictions of initial reactor period, amounts of reactivity (in $) inserted, and yield (in °C). All of these features are categorized as passive since the calculator must depend upon information given it by the operator and its output serves only as a check to the experience of the operator.

4.2 Interrogative/Prohibit Mode

Since the start of operation at the SPR facility, over 12,000 reactor operations have been successfully conducted. However, the increasing complexity of experiments with the associated demands on reactor operation requires that the method of instrument monitoring, data evaluation, and reactor set up be improved to a level complementary to the complexity of experiments. Utilization of the calculator for this type of diagnostic work provides the reactor operator with a significantly improved real time experiment/reactor evaluation tool. This has the additional benefit that the calculator system itself can be easily reevaluated and updated to meet the current demands.

At present, the number of indicators on the reactor console has increased to more than 250 so that monitoring reactor parameters and taking appropriate action is a demanding job and, as noted, this number will increase. The calculator system can have a place in this process by prompting the operator with visual and audible cues. In a typical burst sequence, for instance, it would be valuable to generate caution signals for downward changes in reactor temperature between the time of measurement of burst rod worth and the moment of pulse initiation. With rod position data fed to the calculator, it would be also possible to display a warning whenever a preburst rod correction added reactivity beyond preestablished limits. Furthermore, the operator could be made aware of any drifting of control rods during a wait period by programming the calculator to scan rod position data. Backup scanning could also be performed on safety block position indication, nitrogen temperature and pressure, reactor power and temperature during steady-state operation, scram magnet current, the status of the program and sequential timers, radiation monitors, ventilation exhaust fan performance, shield and ground fault systems, as well as the power supplies associated with all reactor operations. Were this to take place continuously, the potential for operator oversight would be minimized. Such a scheme can be legitimately characterized as "interrogative" since it requires the calculator to sample and investigate a broad range of sensor information. In addition, the software can be arranged to interrogate the operator when decisions have been made which result in caution signals.

It is conceivable that conditions could exist which would need more than caution flags. By way of example, it is possible to perform a period measurement without withdrawing a control rod from its delayed critical position. The consequence would be a burst instead of the sub-prompt critical minipulse: since the entire worth of the burst rod would be inserted above delayed critical. Defense against such an event is possible by creating software that would incorporate the standard reactor operating procedures and prohibit the continuance of a procedure out of

sequence. The use of such calculator-regulated operation would serve as an operator aid to prevent those situations which can result from violations of approved operating procedures. Rather than limit flexibility, such a capability would provide additional assurance that the boundaries defined by the approved Technical Specifications are not exceeded.

References

[1]B. F. Estes, and J. A. Snyder, Sandia Pulsed Reactor Facility (SPRF) Experimenters Manual, Sandia Laboratories, (SAND 79-0391, June 1979).

[2]D. L. Hetrick, Dynamics of Nuclear Reactors, (Chicago: The University of Chicago Press, 1971).